ISSN 1330–0008
CODEN FIZAE4

POLAR INTERFACE OPTICAL OSCILLATION AND FRÖHLICH ELECTRON–PHONON INTERACTION HAMILTONIANS IN A n-LAYER COUPLING QUANTUM WELL

LI ZHANG[a,1] and HONG-JING XIE[b]

[a]*Department of Mechanism and Electron, Panyu Polytechnic, Panyu 511483, P. R. China*
E-mail address: zhangli-gz@263.net Tel.: +86-20-34514451(H); +86-20-86237563(O)

[b]*Department of Physics, Guihuagang Campus, Guangzhou University, Guangzhou 510405, P. R. China*

Received 20 November 2002; revised manuscript received 9 June 2003
Accepted 23 June 2003 Online 20 September 2003

Under dielectric continuum approximation and by using determinant method, the interface optical (IO) phonon modes, the orthogonal relation for polarization vector and electron – IO phonon Fröhlich interaction Hamiltonian in a n-layer coupling quantum well have been derived. Numerical calculations on seven-layer $Al_xGa_{1-x}As/GaAs$ systems have been performed. The IO phonon dispersion relation and the electron – IO phonon coupling function are discussed. Based on the numerical results in this and previous work, general characteristics of the IO phonon modes in a n-layer coupling quantum well system are deduced. The present investigations can be regarded as a generalization of previous studies.

PACS numbers: 74.25.Kc; 71.38.-k; 63.20.Kr UDC 538.971

Keywords: multi-layer coupling quantum well, seven-layer $Al_xGa_{1-x}As/GaAs$ systems, interface optical phonon modes and dispersion relation

1. Introduction

Since the pioneering works of Fuchs and Kliewer [1] and Licari and Evrard [2] on the investigations of polar vibration modes in multi-layer quantum well (QW) structures, many authors [3–15] have shown a great interest in studying phonon modes and electron–phonon interaction in various quantum systems of different geometri-

[1]Corresponding author

cal shapes and dimensionality. The reason for this interest lies in the importance of the electron–phonon interactions in determining the properties related to physical processes, such as transport processes or electron relaxation in confined systems. The physical properties related to polarized phonons are useful for some device applications. For example, the scattering of electrons by optical phonons represents a dominant mechanism of various properties. The electron–phonon interaction and scattering govern a number of important properties of heterostructures, including hot-electron relaxation rates, intersubband transition rates, room-temperature exciton lifetimes, etc. The polaronic effects can also strongly affect the optical and transport properties of the heterostructures.

In order to describe the polar optical oscillations in a semiconductor structure, several theoretical models have been developed, and the dielectric continuum (DC) approximation gives one of the simple and effective models under certain conditions [3], especially for the description of polaronic effects [4,5]. Therefore, the DC model has been widely used to deal with the electron–phonon interaction in various confined quantum systems. Mori and Ando [6] investigated the phonon modes in single and double heterostructures within the framework of DC, and discussed the dispersion frequencies of interface optical (IO) phonon versus wave vector. Chen et al. [7] studied optical phonon modes in a double heterostructure of polar crystals by solving the equation of motion for the polarization vector, and found that there exist four branches of IO phonon in the system. Before investigating the transport properties in $Al_xGa_{1-x}As/GaAs$ single heterostructures, Bordone and Lugli [8] obtained the IO phonon modes in the system, and the potential distributions of IO phonons were discussed. In recent years, within the DC model, Shi et al. [9–13] calculated the interface and surface optical (SO) phonon modes and the corresponding electron–phonon Hamiltonians in multi-layer QW systems having three to five layers. Both the finite and infinite boundary width were investigated, and they mainly discussed the dispersion relations and the electrostatic potential distribution for the SO and IO phonon modes. By using the method of diagonalization of the equations of motion for inertial polarization vectors in the finite basis, Klimin et al. [14] calculated the phonon eigenmodes and electron–phonon interaction in multilayer structures, but the group only did the numerical calculations on three-layer symmetrical QW structures, and the general characteristics of the IO phonon modes were not considered.

In the present paper, using the determinant method as in our recent work [15], we have derived the IO phonon modes and electron–phonon interaction Hamiltonian in a n-layer coupling QW system under DC approximation. The method of dealing with the multilayer structures in the present study is somewhat different from that of Ref. [14]. In Ref. [14], the authors adopted the method of diagonalization of the equations of motion for inertial polarization vectors in the finite basis. The determinant method described in the present paper is basically the method of solving linear equations. The determinant method has the advantage of easy and direct calculation, and it applies to investigations of electronic states or optical phonon modes in multi-layer quantum systems [15]. The main advantage of this study is the following. The orthonormal relation for the polarization vector of IO

modes in a quantum system with an arbitrary number of layers has been derived. The Fröhlich electron–phonon interaction Hamiltonian has been obtained from the orthonormal relation and the dynamic equation of motion of the crystal lattice. For the classic $Al_xGa_{1-x}As/GaAs$ materials, the IO phonon dispersion relation and the phonon potential distributions for seven-layer coupling QW have been computed and discussed. The general characteristics of IO phonon for a n-layer QW system have been deduced from the results obtained in previous studies and the discussion in this study.

The main reasons why the seven-layer coupling QW system was chosen to perform the numerical calculation are as follows: i) to our knowledge, the two- to five-layer heterostructure systems have been investigated [6–13], but the seven-layer heterostructure system has not been treated previously, ii) the features of IO phonon modes in two- to five-layer heterostructure systems can be obtained by simplifying the seven-layer coupling QW system [10–13], iii) the discussion of the seven-layer system and of the results obtained in fixed layer-number heterostructure systems [6–13] allows the deduction of the general characteristics of the IO phonon modes in a n-layer coupling QW system, iv) in order to verify the validity of the determinant method, we developed the treatment of phonon modes in multi-layer coupling QWs, so the seven-layer coupling QW system was chosen. Moreover, the results obtained in this paper should be very useful for further experimental and theoretical studies of the electron–phonon interaction and scattering in multilayer QW structures. For example, polaronic effects on the intersubband optical absorption for a mid-infrared field with z-component and the inelastic light scattering by phonon excitations with the usual backscattering geometry.

2. Theory

Within the framework of DC approximation and taking the phonon potential couplings between the IO phonon modes into account, the IO phonon potential in the n-layer coupling QW system can be written as

$$\phi_{\mathbf{q}}^{\mathrm{IO}}(\mathbf{r}) = \begin{cases} A_0 e^{q_z z} e^{\mathrm{i}\mathbf{Q}\cdot\rho} & -\infty < z \le z_0 \\ (A_1 e^{q_z z} + B_1 e^{-q_z z}) e^{\mathrm{i}\mathbf{Q}\cdot\rho} & z_0 < z \le z_1 \\ \ldots & \ldots \\ (A_i e^{q_z z} + B_i e^{-q_z z}) e^{\mathrm{i}\mathbf{Q}\cdot\rho} & z_{i-1} < z \le z_i \\ \ldots & \ldots \\ (A_{n-1} e^{q_z z} + B_{n-1} e^{-q_z z}) e^{\mathrm{i}\mathbf{Q}\cdot\rho} & z_{n-2} < z \le z_{n-1} \\ B_n e^{-q_z z} e^{\mathrm{i}\mathbf{Q}\cdot\rho} & z_{n-1} < z < \infty \end{cases} , \qquad (1)$$

where

$$\begin{aligned} \mathbf{Q} &= \mathbf{q} - q_z \mathbf{k} = q_x \mathbf{i} + q_y \mathbf{j} , \qquad (2) \\ \rho &= x\mathbf{i} + y\mathbf{j} . \end{aligned}$$

Because the IO phonon potential functions should satisfy the Laplace equation $\nabla^2\phi^{\rm IO}_{\mathbf{q}}(\mathbf{r}) \equiv 0$, the following relation is obtained,

$$q_z^2 = q_x^2 + q_y^2 \,. \tag{3}$$

The continuity of the phonon potential functions and the normal components of the electric displacement at $z = z_i$ ($i = 0, 1, ..., n-1$) imply

$$\begin{cases} \phi^{\rm IO}_{i\mathbf{q}}|_{z=z_i} = \phi^{\rm IO}_{i+1,\mathbf{q}}|_{z=z_i} \\ \varepsilon_i(\omega)\dfrac{\partial\phi^{\rm IO}_{i\mathbf{q}}}{\partial z}|_{z=z_i} = \varepsilon_{i+1}(\omega)\dfrac{\partial\phi^{\rm IO}_{i+1,\mathbf{q}}}{\partial z}|_{z=z_i} \end{cases} , \; i = 0,\ 1,\ ...\ n-1 \tag{4}$$

with the dielectric function $\varepsilon_i(\omega)$ of the ith material given by

$$\varepsilon_i(\omega) = \varepsilon_{i\infty}\frac{\omega^2 - \omega^2_{{\rm LO}i}}{\omega^2 - \omega^2_{{\rm TO}i}} \;,\; i = 0,\ 1,\ ...\ n\,, \tag{5}$$

where $\varepsilon_{i\infty}$ is the high-frequency dielectric constant of ith layer material, $\omega_{{\rm TO}i}$ and $\omega_{{\rm LO}i}$ are the corresponding frequencies of the transverse-optical and longitudinal-optical vibrations, respectively. We define

$$\begin{aligned} &\varepsilon_i \exp(q_z z_i) = f_i \,, && \varepsilon_{i+1}\exp(q_z z_i) = f_i' \,, \\ &\varepsilon_i \exp(-q_z z_i) = g_i \,, && \varepsilon_{i+1}\exp(-q_z z_i) = g_i' \,, \\ &\exp(q_z z_i) = h_i \,, && \exp(-q_z z_i) = h_i^{-1} \,. \end{aligned} \tag{6}$$

Then the dispersion relation of IO phonons is obtained via the $2n \times 2n$ determinant

$$\begin{vmatrix} h_0 & -h_0 & -h_0^{-1} & 0 & 0 & 0 & 0 & 0 & 0 & 0 & 0 \\ f_0 & -f_0' & g_0' & 0 & 0 & 0 & 0 & 0 & 0 & 0 & 0 \\ 0 & h_1 & h_1^{-1} & -h_1 & -h_1^{-1} & 0 & 0 & 0 & 0 & 0 & 0 \\ 0 & f_1 & -g_1 & -f_1' & g_1' & 0 & 0 & 0 & 0 & 0 & 0 \\ 0 & 0 & 0 & 0 & 0 & ... & 0 & 0 & 0 & 0 & 0 \\ 0 & 0 & 0 & 0 & 0 & 0 & h_{n-2} & h_{n-2}^{-1} & -h_{n-2} & -h_{n-2}^{-1} & 0 \\ 0 & 0 & 0 & 0 & 0 & 0 & f_{n-2} & -g_{n-2} & -f_{n-2}' & g_{n-2}' & 0 \\ 0 & 0 & 0 & 0 & 0 & 0 & 0 & 0 & h_{n-1} & h_{n-1}^{-1} & -h_{n-1}^{-1} \\ 0 & 0 & 0 & 0 & 0 & 0 & 0 & 0 & f_{n-1} & -g_{n-1} & g_{n-1}' \end{vmatrix} = 0 \,. \tag{7}$$

Substituting Eq. (5) into the above determinant, the frequencies of IO phonon could be solved. After evaluationg ω, the dielectric functions $\varepsilon_i(\omega)$ follow from Eq. (5). By using Eqs. (4), A_i and B_i ($i = 1, 2$ to n) can be expressed as

$$\begin{cases} A_i = \dfrac{M_{2i-1}}{M_0}A_0 \\ B_i = \dfrac{M_{2i}}{M_0}A_0 \end{cases} , i = 1,\ 2\ ,\ ...\ n-1\,, \tag{8}$$

$$B_n = \frac{M_{2n-1}}{M_0} A_0 \,, \tag{9}$$

$$B_0 = A_n = 0 \tag{10}$$

with

$$M_0 = \begin{vmatrix} -h_0 & -h_0^{-1} & 0 & 0 & 0 & 0 & 0 & 0 & 0 & 0 \\ -f_0' & g_0' & 0 & 0 & 0 & 0 & 0 & 0 & 0 & 0 \\ h_1 & h_1^{-1} & -h_1 & -h_1^{-1} & 0 & 0 & 0 & 0 & 0 & 0 \\ f_1 & -g_1 & -f_1' & g_1' & 0 & 0 & 0 & 0 & 0 & 0 \\ 0 & 0 & 0 & 0 & ... & 0 & 0 & 0 & 0 & 0 \\ 0 & 0 & 0 & 0 & 0 & h_{n-2} & h_{n-2}^{-1} & -h_{n-2} & -h_{n-2}^{-1} & 0 \\ 0 & 0 & 0 & 0 & 0 & f_{n-2} & -g_{n-2} & -f_{n-2}' & g_{n-2}' & 0 \\ 0 & 0 & 0 & 0 & 0 & 0 & 0 & h_{n-1} & h_{n-1}^{-1} & -h_{n-1}^{-1} \end{vmatrix}, \tag{11}$$

$$M_j = \begin{vmatrix} -h_0 & -h_0^{-1} & 0 & 0 & -h_0 & 0 & 0 & 0 & 0 & 0 \\ -f_0' & g_0' & 0 & 0 & -f_0 & 0 & 0 & 0 & 0 & 0 \\ h_1 & h_1^{-1} & -h_1 & -h_1^{-1} & 0 & 0 & 0 & 0 & 0 & 0 \\ f_1 & -g_1 & -f_1' & g_1' & 0 & 0 & 0 & 0 & 0 & 0 \\ 0 & 0 & 0 & 0 & ... & 0 & 0 & 0 & 0 & 0 \\ 0 & 0 & 0 & 0 & 0 & h_{n-2} & h_{n-2}^{-1} & -h_{n-2} & -h_{n-2}^{-1} & 0 \\ 0 & 0 & 0 & 0 & 0 & f_{n-2} & -g_{n-2} & -f_{n-2}' & g_{n-2}' & 0 \\ 0 & 0 & 0 & 0 & 0 & 0 & 0 & h_{n-1} & h_{n-1}^{-1} & -h_{n-1}^{-1} \end{vmatrix}, \tag{12}$$

where M_0 and M_j are $(2n-1)\times(2n-1)$ determinants. It should be noticed that the column matrix $(-h_0, -f_0, 0, 0, ..., 0, 0, 0)$ is located at the jth column in M_j. During the calculation procedure, the Cramer rule for solving the linear equations was employed. Using Eqs. (8), (9) and (10), the phonon potential function (1) can be rewritten as

$$\phi_{\mathbf{q}}^{\mathrm{IO}}(\mathbf{r}) = \begin{cases} A_0 M_0 e^{q_z z} e^{i\mathbf{Q}\cdot\rho} & -\infty < z \le z_0 \\ A_0 (M_1 e^{q_z z} + M_2 e^{-q_z z}) e^{\mathrm{i}\mathbf{Q}\cdot\rho} & z_0 < z \le z_1 \\ ... & ... \\ A_0 (M_{2i-1} e^{q_z z} + M_{2i} e^{-q_z z}) e^{\mathrm{i}\mathbf{Q}\cdot\rho} & z_{i-1} < z \le z_i \\ ... & ... \\ A_0 (M_{2n-3} e^{q_z z} + M_{2n-2} e^{-q_z z}) e^{\mathrm{i}\mathbf{Q}\cdot\rho} & z_{n-2} < z \le z_{n-1} \\ A_0 M_{2n-1} e^{-q_z z} e^{\mathrm{i}\mathbf{Q}\cdot\rho} & z_{n-1} < z < \infty \,. \end{cases} \tag{13}$$

So, the polarization fields for the IO phonon modes of the system are given as

$$\mathbf{P}_{\mathbf{q}}^{\mathrm{IO}} = \frac{1-\varepsilon}{4\pi}\nabla\phi_{\mathbf{q}}^{\mathrm{IO}}(\mathbf{r}) = \frac{A_0 e^{\mathrm{i}\mathbf{Q}\cdot\rho}}{4\pi}\times \tag{14}$$

$$\begin{cases} (1-\varepsilon_0)M_0 e^{q_z z}(\mathrm{i}q_x\mathbf{i}+\mathrm{i}q_y\mathbf{j}+q_z\mathbf{k}) & -\infty < z \le z_0 \\ (1-\varepsilon_1)[\mathrm{i}q_x(M_1e^{q_z z}+M_2e^{-q_z z})\mathbf{i}+\mathrm{i}q_y(M_1e^{q_z z} & \\ +M_2e^{-q_z z})\mathbf{j}+q_z(M_1e^{q_z z}-M_2e^{-q_z z})\mathbf{k}] & z_0 < z \le z_1 \\ \ldots & \ldots \\ (1-\varepsilon_i)[\mathrm{i}q_x(M_{2i-1}e^{q_z z}+M_{2i}e^{-q_z z})\mathbf{i}+\mathrm{i}q_y(M_{2i-1}e^{q_z z} & \\ +M_{2i}e^{-q_z z})\mathbf{j}+q_z(M_{2i-1}e^{q_z z}-M_{2i}e^{-q_z z})\mathbf{k}] & z_{i-1} < z \le z_i \\ \ldots & \ldots \\ (1-\varepsilon_{n-1})[\mathrm{i}q_x(M_{2n-3}e^{q_z z}+M_{2n-2}e^{-q_z z})\mathbf{i}+\mathrm{i}q_y(M_{2n-3}e^{q_z z} & \\ +M_{2n-2}e^{-q_z z})\mathbf{j}+q_z(M_{2n-3}e^{q_z z}-M_{2n-2}e^{-q_z z})\mathbf{k}] & z_{n-2} < z \le z_{n-1} \\ (1-\varepsilon_n)M_{2n-1}e^{-q_z z}(\mathrm{i}q_x\mathbf{i}+\mathrm{i}q_y\mathbf{j}-q_z\mathbf{k}) & z_{n-1} < z < \infty\,. \end{cases}$$

Then we obtain the orthogonal relation for $\mathbf{P}_{\mathbf{q}}^{\mathrm{IO}}$

$$\begin{aligned} &\int \mathbf{P}_{\mathbf{q}'}^{\mathrm{IO}\,*}\cdot\mathbf{P}_{\mathbf{q}}^{\mathrm{IO}}\mathrm{d}^3\mathbf{r} \\ =\ & \frac{S\,|A_0|^2\,q_z}{16\pi^2}\Big\{\sum_{i=1}^{n-1}(1-\varepsilon_i)^2[M_{2i-1}^2(e^{2q_z z_i}-e^{2q_z z_{i-1}})-M_{2i}^2(e^{-2q_z z_i}-e^{-2q_z z_{i-1}})] \\ & +(1-\varepsilon_0)^2M_0^2+(1-\varepsilon_n)^2M_{2n-1}^2e^{-2q_z z_{n-1}}\Big\}\delta_{q_z' q_z}\delta(\mathbf{Q}'-\mathbf{Q})\,, \end{aligned} \tag{15}$$

where S is the area of the cross section parallel to the xy-plane.

The Hamiltonian for the IO phonon modes is given as [4,5]

$$\begin{aligned} H_{\mathrm{IO}} \ =\ & \frac{1}{2}\int\Big[n^*\mu\Big(\frac{1}{n^*e[1+(\alpha\mu/e^2)(\omega_0^2-\omega^2)]}\Big)^2\,\dot{\mathbf{P}}^*\cdot\mathbf{P} \\ & +n^*\mu\omega^2\Big(\frac{1}{n^*e[1+(\alpha\mu/e^2)(\omega_0^2-\omega^2)]}\Big)^2\mathbf{P}^*\cdot\mathbf{P}\Big]\mathrm{d}^3\mathbf{r}\,, \end{aligned} \tag{16}$$

where μ is the reduced mass of the ion pair, ω_0 is the frequency associated with the short-range force between ions, n^* is the number of ion pairs per unit volume, and α is the electronic polarizability per ion pair.

Using the orthogonal relation of the polarization vector (15), we obtain

$$\begin{aligned} |A_0|^{-2} &= \frac{Sq_z}{2\pi\omega^2}\Big\{\Big(\frac{1}{\varepsilon_0-\varepsilon_{00}}-\frac{1}{\varepsilon_0-\varepsilon_{0\infty}}\Big)^{-1}M_0^2+\Big(\frac{1}{\varepsilon_n-\varepsilon_{n0}}-\frac{1}{\varepsilon_n-\varepsilon_{n\infty}}\Big)^{-1} \\ &\times M_{2n-1}^2 e^{-2q_z z_{n-1}}+\sum_{i=1}^{n-1}\Big[\Big(\frac{1}{\varepsilon_i-\varepsilon_{i0}}-\frac{1}{\varepsilon_i-\varepsilon_{i\infty}}\Big)^{-1} \\ &\times[M_{2i-1}^2(e^{2q_z z_i}-e^{2q_z z_{i-1}})-M_{2i}^2(e^{-2q_z z_i}-e^{-2q_z z_{i-1}})]\Big]\Big\}. \end{aligned} \tag{17}$$

Then $\mathbf{P}_{\mathbf{q}}^{\mathrm{IO}}$ form orthonormal and complete sets, which can be used to express the IO phonon field H_{IO} and the electron–phonon interaction Hamiltonian $H_{\mathrm{e-IO}}$. The IO phonon field is given as

$$H_{\mathrm{IO}}=\sum_{q_z,\mathbf{Q}}\hbar\omega\Big[b_{q_z}^{\dagger}(\mathbf{Q})b_{q_z}(\mathbf{Q})+\frac{1}{2}\Big], \tag{18}$$

where $b_{q_z}^{\dagger}(\mathbf{Q})$ and $b_{q_z}(\mathbf{Q})$ are creation and annihilation operators for IO phonon of the (q_z, $\mathbf{Q}$)th mode. They satisfy the commutative rules for bosons

$$\begin{aligned} [b_{q_z}(\mathbf{Q}),b_{q_z'}^{\dagger}(\mathbf{Q}')] &= \delta_{q_z' q_z}\delta(\mathbf{Q}'-\mathbf{Q}), \\ [b_{q_z}(\mathbf{Q}),b_{q_z'}(\mathbf{Q}')] &= [b_{q_z}^{\dagger}(\mathbf{Q}),b_{q_z'}^{\dagger}(\mathbf{Q}')]=0. \end{aligned} \tag{19}$$

The Fröhlich Hamiltonian describing the interaction between the electron and the IO phonon is given by

$$H_{\mathrm{e-IO}}=-\sum_{q_z,\mathbf{Q}}\Gamma_{q_z}^{\mathrm{IO}}(z)[e^{\mathrm{i}\mathbf{Q}\cdot\rho}b_{q_z}(\mathbf{Q})+\mathrm{H.c.}], \tag{20}$$

where the coupling function $\Gamma_{q_z}^{\mathrm{IO}}(z)$ is defined as

$$\Gamma_{q_z}^{\mathrm{IO}}(z)=N_{q_z}\times\begin{cases} M_0e^{q_z z} & -\infty<z\le z_0 \\ (M_1e^{q_z z}+M_2e^{-q_z z}) & z_0<z\le z_1 \\ \ldots & \ldots \\ (M_{2i-1}e^{q_z z}+M_{2i}e^{-q_z z}) & z_{i-1}<z\le z_i \\ \ldots & \ldots \\ (M_{2n-3}e^{q_z z}+M_{2n-2}e^{-q_z z}) & z_{n-2}<z\le z_{n-1} \\ M_{2n-1}e^{-q_z z} & z_{n-1}<z<\infty, \end{cases} \tag{21}$$

with

$$
\begin{aligned}
|N_{q_z}|^2 &= |A_0|^2 \frac{\hbar e^2}{\omega} \\
&= \frac{2\pi\hbar\omega e^2}{Sq_z}\Big\{\Big(\frac{1}{\varepsilon_0-\varepsilon_{00}}-\frac{1}{\varepsilon_0-\varepsilon_{0\infty}}\Big)^{-1}M_0^2+\Big(\frac{1}{\varepsilon_n-\varepsilon_{n0}}-\frac{1}{\varepsilon_n-\varepsilon_{n\infty}}\Big)^{-1} \\
&\quad \times M_{2n-1}^2 e^{-2q_z z_{n-1}}+\sum_{i=1}^{n-1}\Big[\Big(\frac{1}{\varepsilon_i-\varepsilon_{i0}}-\frac{1}{\varepsilon_i-\varepsilon_{i\infty}}\Big)^{-1}\times \\
&\quad [M_{2i-1}^2(e^{2q_z z_i}-e^{2q_z z_{i-1}})-M_{2i}^2(e^{-2q_z z_i}-e^{-2q_z z_{i-1}})]\Big]\Big\}^{-1}. \qquad (22)
\end{aligned}
$$

3. Results and discussion

Numerical calculations were carried out on the seven-layer $Al_{0.1}Ga_{0.9}As$/-$Al_{0.25}Ga_{0.75}As$/$Al_{0.35}Ga_{0.65}As$/ GaAs/$Al_{0.15}Ga_{0.85}As$/$Al_{0.3}Ga_{0.7}As$/$Al_{0.4}Ga_{0.6}As$ system with thicknesses ∞ / 8 nm / 6 nm / 3 nm / 4 nm / 5 nm / ∞. The calculations were mainly focused on dispersion relations of IO phonon and the coupling functions of electron – IO phonon interaction. The material parameters [16] are listed in Table 1 and the scheme of our model is given in Fig. 1.

TABLE 1. The material parameters [16].

	GaAs	$Ga_{1-x}Al_xAs$	AlAs
$\hbar\omega_{\mathrm{LO}}$ (meV)	36.25	$36.25+3.83x+17.12x^2-5.11x^3$	50.09
$\hbar\omega_{\mathrm{TO}}$ (meV)	33.29	$33.29+10.70x+0.03x^2+0.86x^3$	44.88
ϵ_0	13.18	$3.18-3.12x$	10.06
ϵ_∞	10.89	$10.89-2.73x$	8.16

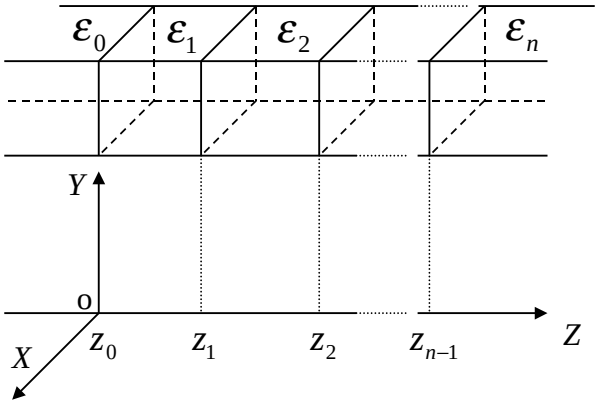

Fig. 1. The schematic structure of the n-layer coupling quantum well system.

Figure 2 shows the IO phonon dispersion frequencies versus the wave vectors in the z-direction of the seven-layer coupling QW system. It can be seen that, there exist twelve branches of IO phonon modes in the system, i.e., two branches on each interface. The dispersions of the twelve modes are obvious only when $q_z < 0.1$ nm^{-1}, but the dispersions are negligible when $q_z > 0.2$ nm^{-1}, namely, each mode approaches a certain frequency value. Detailed calculation have shown, when $q_z \to 0$, the frequencies of the twelve branches of IO phonon approach ω_{TO3}, ω_{TO4}, ω_-, ω_{TO1}, ω_{LO3}, ω_{TO5}, ω_{TO2}, ω_{LO4}, ω_{LO1}, ω_{LO5}, ω_+, and ω_{LO2} in terms of the order of increasing frequency. We notice that ω_{LO0}, ω_{TO0}, ω_{TO6} and ω_{LO6} are forbidden, but two new frequencies ω_+ and ω_- appear. Furthermore, it can be seen that $\omega_{\mathrm{TO0}} < \omega_- < \omega_{\mathrm{LO0}}$ and $\omega_{\mathrm{TO6}} < \omega_+ < \omega_{\mathrm{LO6}}$. This result is completely due to the asymmetry of the seven-layer system [10]. When the mole fractions of Al, x, in the outermost materials (the 6th and 0th layers) are the same, this frequency-forbidden behaviour disappears [6,10], namely, $\omega_+ = \omega_{\mathrm{LO6}}$ (ω_{LO0}) and $\omega_- = \omega_{\mathrm{TO6}}$ (ω_{TO0}).

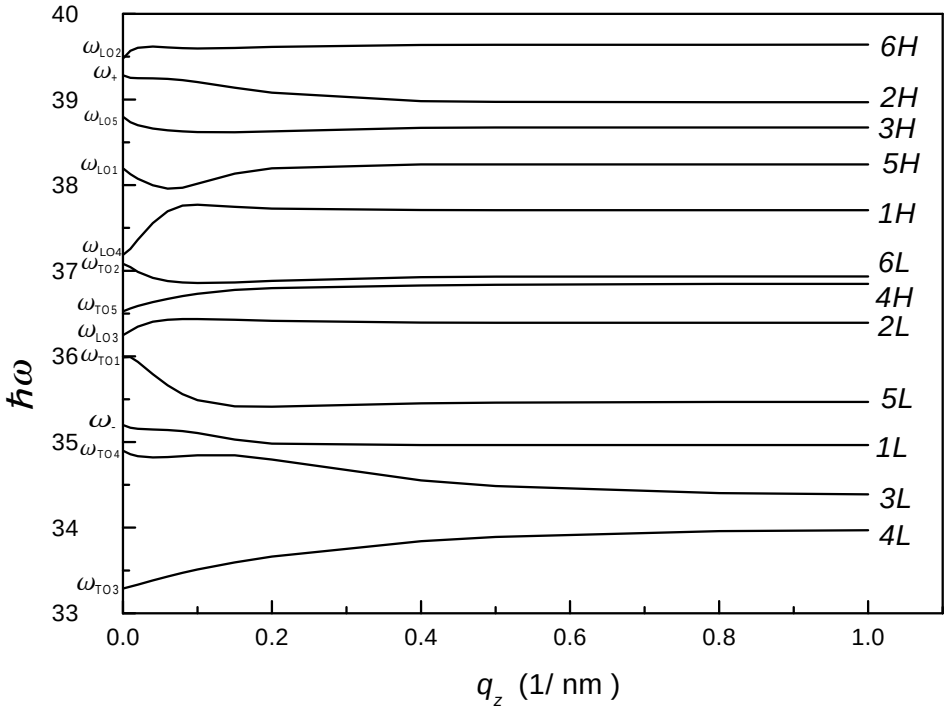

Fig. 2. Dispersion curves of the IO phonon modes for the seven-layer QW with thicknesses ∞ / 8 nm / 6 nm / 3 nm / 4 nm / 5 nm / ∞.

In order to distinguish and label the twelve branches of IO phonon modes, the limit frequencies of IO phonon when $q_z \to \infty$ in the single planar heterostructure [6,8] formed by the two materials on both sides of the six interfaces are listed in

Table 2. According to Table 2, it is easy to label the twelve IO phonon modes in Fig. 2. For example, 4H and 4L denote the two modes mainly localized in the vicinity of the fourth interface, and they represent the higher-frequency branch and lower-frequency branch at the fourth interface, respectively.

TABLE 2. The limit frequencies of the IO phonon modes in single heterostructures. The branch with lower frequency is labeled by $\hbar\omega_{i\mathrm{L}}$, the branch with higher frequency is labeled by $\hbar\omega_{i\mathrm{H}}$, and the index i denotes the ith interface.

Interface materials	$\hbar\omega_{i\mathrm{L}}$ (meV)	$\hbar\omega_{i\mathrm{H}}$ (meV)
$Al_{0.1}Ga_{0.9}As/Al_{0.25}Ga_{0.75}As$ $(i=1)$	34.96	37.71
$Al_{0.25}Ga_{0.75}As/Al_{0.35}Ga_{0.65}As$ $(i=2)$	36.39	38.97
$Al_{0.35}Ga_{0.65}As/GaAs$ $(i=3)$	34.38	38.67
$GaAs/Al_{0.15}Ga_{0.85}As$ $(i=4)$	33.97	36.85
$Al_{0.15}Ga_{0.85}As/Al_{0.3}Ga_{0.7}As$ $(i=5)$	35.47	38.24
$Al_{0.3}Ga_{0.7}As/Al_{0.4}Ga_{0.6}As$ $(i=6)$	36.93	39.64

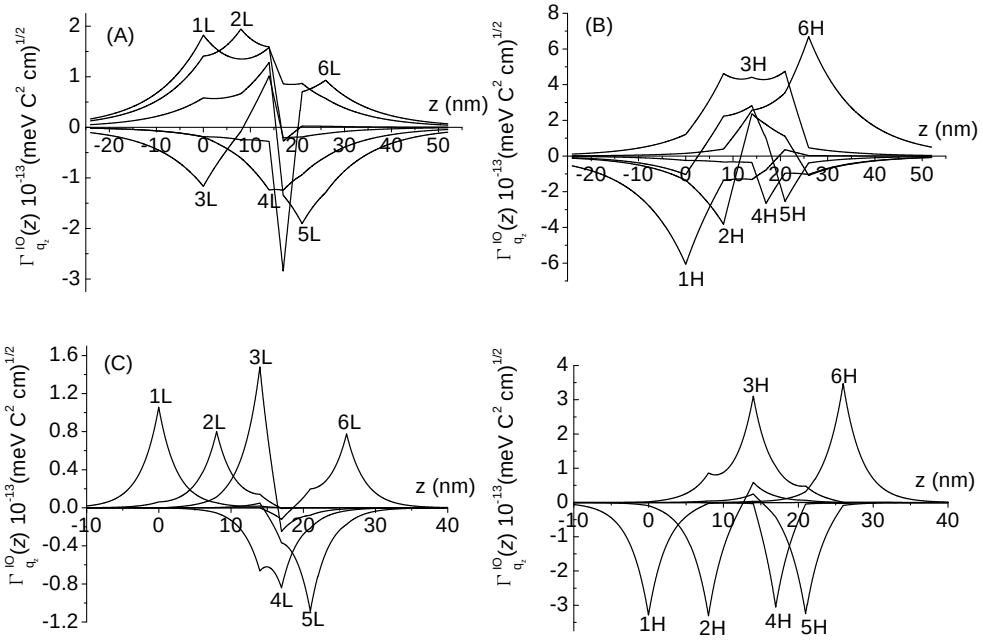

Fig. 3. The coupling functions $\Gamma^{\mathrm{IO}}_{q_z}(z)$ as functions of z for: A) and B) $q_z = 0.1$ nm^{-1} and C) and D) $q_z = 0.4$ nm^{-1}.

Figure 3 shows the electron – IO phonon coupling functions $\Gamma^{\mathrm{IO}}_{q_z}(z)$ as functions of z. In fact, Fig. 3A and Fig. 3B correspond to $q_z = 0.1$ nm^{-1}, and Fig. 3C and Fig. 3D correspond to $q_z = 0.4$ nm^{-1}. One can see from the figure that, when q_z is small (such as 0.1 nm^{-1}), the functions $\Gamma^{\mathrm{IO}}_{q_z}(z)$ for each mode at the interfaces are relatively evenly distributed [15], namely, the peaks in the curves at each interface are not very sharp. But when q_z is large (such as 0.4 nm^{-1}), the functions $\Gamma^{\mathrm{IO}}_{q_z}(z)$ of modes iL and iH ($i = 1, 2, ..., 6$) tend to be localized more and more at the ith interface, namely, the sharpest peak in each curve only appears at the ith interface and the peaks at the other interfaces almost disappear, so that the two frequencies approach the frequencies in single heterostructure. These characteristics just prove the results in Table 2. Comparing Fig. 3A with Fig. 3B or Fig. 3C with Fig. 3D, we can see that the couplings of six branches of IO phonon with higher frequencies (iH branches) are stronger than those with lower frequencies (iL branches). Comparing Fig. 3A with Fig. 3C or Fig. 3B with Fig. 3D, we found that, with the increasing of q_z, the coupling of each IO mode becomes weaker and weaker, which can be seen clearly in Fig. 4.

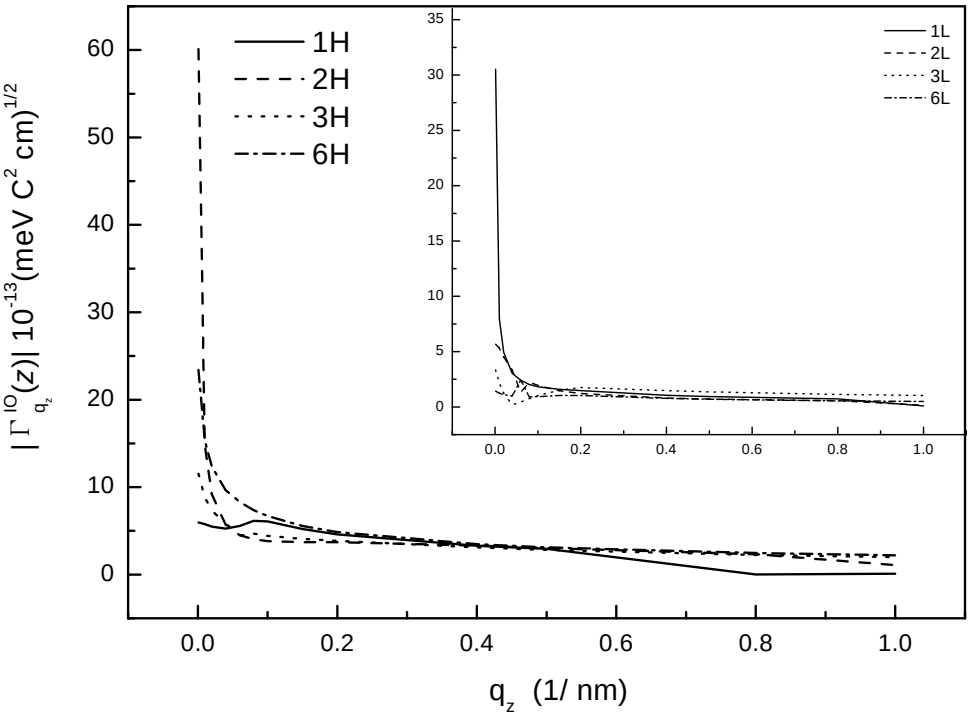

Fig. 4. The absolute values $\left|\Gamma^{\mathrm{IO}}_{q_z}(z)\right|$ as functions of q_z for the eight branches of IO phonon modes: the outer figure is for modes 1H, 2H, 3H and 6H, and the embedded figure for modes 1L, 2L, 3L and 6L.

The absolute values $\left|\Gamma_{q_z}^{\mathrm{IO}}(z)\right|$ as functions of q_z for the eight branches of IO phonon modes are plotted in Fig. 4. In fact, the outer figure is for 1H, 2H, 3H and 6H, and the embedded figure is for 1L, 2L, 3L and 6L. According to the discussion of Fig. 3, $z = 0$, 14, 8 and 26 nm were chosen for the four branches of IO phonon modes 1H (1L), 2H (2L), 3H (3L) and 6H (6L), respectively. It is seen that, as q_z is small (such as 0.2 nm^{-1}), the $\left|\Gamma_{q_z}^{\mathrm{IO}}(z)\right|$ for the modes 1H, 2L, 3L and 6L reveal slight oscillatory behaviour, but when q_z is over 0.2 nm^{-1}, the $\left|\Gamma_{q_z}^{\mathrm{IO}}(z)\right|$ for each mode decreases monotonously with the increasing of q_z. A similar behaviour for each mode for higher values of q_z is found because, for higher q_z, the polarized zone is smaller (refer to Fig. 3), and the electron – IO phonon interaction becomes weaker. Comparing the modes iH with iL (i = 1, 2, 3 and 6), it is found that electron – IO phonon coupling for the higher-frequency branch is more important than that for the lower-frequency branch. Another interesting feature in Fig. 4 is that the strong coupling obtained in the 2H and 1L branches is in the vicinity of the center of the Brillouin zone ($q_z \to 0$). This is because, as $q_z \to 0$, the mode 2H with frequency ω_+ and mode 1L with frequency ω_- may cause a remarkable polarization in media. Thus the frequency-forbidden behaviour of an asymmetric heterostructure has significant influence on the electron–phonon interaction [12,13].

Next, we consider the relations between the theoretical results of IO phonon modes obtained in this paper and some previous results of IO phonon modes in fixed layer-number heterostructure systems. In fact, the work described in this paper can be regarded as a generalization of previous work [6–13], namely, if the corresponding layer-number and material parameters for the heterostructure systems are chosen, the results for the dispersion relations, the electron–coupling functions of the IO phonons in two- to five-layer heterostructure systems can be obtained [6–13]. Moreover, with a little modification, the results on the IO phonon modes in the case of the finite boundary width, such as in Refs. [9] and [11] can also be obtained. Through the analysis of the numerical results in this work and previous work [6-8,10,12-13], it is found that the number of IO phonon modes in the systems is $2(n-1)$ ($n \geq 2$). For example, the number of IO phonon modes in three- [6] and four-layer [10,12] heterosturcture systems are four and six branches, while in the seven-layer system, the number is twelve. Due to the asymmetry of the seven-layer heterostructure system discussed in this paper, the frequency-forbidden behaviour has been observed, which is analogous to the case in Ref. [13].

4. Summary

In the present paper, by using the determinant method, we have deduced the interface-optical (IO) phonon modes in a n-layer coupling QW system within the framework of the dielectric continuum approximation. The orthogonal relation of the polarization vector, dispersion relation and the electron – IO phonon interaction Hamiltonian have been derived. Numerical calculations on a seven-layer system reveal that there are twelve branches of IO phonon modes in the system. When q_z approaches 0, the frequency-forbidden behaviour is observed due to the asymmetry

of the system [10]. When $q_z \to \infty$, each frequency value approaches one of the two frequency values of single heterostructure. This feature is used to distinguish and label these branches of the IO phonon modes. When q_z is small, the spatial distribution of the coupling function $\Gamma^{\mathrm{IO}}_{q_z}(z)$ does not reveal a very sharp peak. With increasing q_z, the spatial distribution of $\Gamma^{\mathrm{IO}}_{q_z}(z)$ tends to be localized at some interface. Furthermore, the coupling magnitude $\left|\Gamma^{\mathrm{IO}}_{q_z}(z)\right|$ becomes smaller and smaller. In the case of weak coupling in multi-layer quantum systems, it seems appropriate to use the perturbation method to investigate the polaron effects as in the case of other low-dimensional heterostructures.

On the basis of the numerical results in this and previous work [6-8,10,12-13], it is reasonable to draw the following conclusions for a n-layer coupling QW system as shown in Fig. 1. The number of IO phonon modes in the system is $2(n-1)$ $(n \geq 2)$. On each interface, there exist two IO phonon modes. The dispersion is obvious only when the wave vector in z-direction is small. With the increase of the wave vector, the dispersion frequency of each mode approaches to the one frequency value of the single heterostructure, which can be used to label the IO phonon modes. Further study revealed that, as the wave vector increases, each IO phonon mode is more and more localized in the vicinity of a certain interface, so that each IO phonon frequency approaches one of the limiting frequency values of the single heterostructure. This work can be regarded as a generalization of previous work [6-14], and it provides an effective method to solve the phonon effects, such as the polaronic effect, the bound polaronic effect and the effect of exciton–phonon interaction in the multi-layer coupling quantum well systems.

Acknowledgements

One of the authors (H. J. Xie) is supported by Guangdong Provincial Natural Science Foundation of China. The authors would also like to acknowledge the detailed and valuable suggestions of the referees.

References

[1] R. Fuchs and K. L. Kliewer, Phys. Rev. A **140** (1965) 2076.

[2] J. Licari and R. Evrard, Phys. Rev. B **15** (1977) 2254.

[3] Kun Huang and Bangfen Zhu, Phys. Rev. B **38** (1988) 13377.

[4] Hong-Jing Xie, Chuan-Yu Chen and Ben-Kun Ma, J. Phys.: Condens. Matter **12** (2000) 8623.

[5] Hong-Jing Xie, Chuan-Yu Chen and Ben-Kun Ma, Phys. Rev. B **61** (2000) 4827.

[6] N. Mori and T. Ando, Phys. Rev. B **40** (1989) 6175.

[7] R. Chen, D. L. Lin and Thomas F. George, Phys. Rev. B **41** (1990) 1435.

[8] P. Bordone and P. Lugli, Phys. Rev. B **49** (1994) 8178.

[9] Shi Jun-jie and Pan Shao-hua, Phys. Rev. B **46** (1992) 4265.

[10] Shi Jun-jie, Ling-xi shangguan and Pan Shao-hua, Phys. Rev. B **47** (1993) 13471.

[11] Shi Jun-jie and Pan Shao-hua, Acta Phys. Sin. **43** (1994) 790.

[12] Shi Jun-jie and Pan Shao-hua, Phys. Rev. B **51** (1995) 17681.

[13] Shi Jun-jie and Pan Shao-hua, J. Appl. Phys. **80** (1996) 3863.

[14] S. N. Klimin, E. P. Pokatilov and V. M. Fomin, phys. stat. sol. (b) **190** (1995) 441.

[15] L. Zhang, H. J. Xie and C. Y. Chen, Eur. Phys. J. B **27** (2002) 577.

[16] S. Adachi, J. Appl. Phys. **58** (1985) R1.

POLARNE GRANIČNE OPTIČKE OSCILACIJE I FRÖHLICHOVI HAMILTONIJANI S ELEKTRONSKO-FONONSKIM MEĐUDJELOVANJEM U n-SLOJNOJ VEZANOJ KVANTNOJ JAMI

U približenju dielektričnog kontinuuma i primjenom determinantne metode, izveli smo granične optičke (GO) fononske modove, relaciju za ortogonalnost polarizacijskog vektora i Fröhlichov hamiltonijan s elektronsko-fononskim međudjelovanjem za n-slojnu vezanu kvantnu jamu. Proveli smo numeričke račune za sedmoslojni sustav $Al_xGa_{1-x}As/GaAs$. Raspravljamo GO fononsku disperzijsku relaciju i funkciju vezanja elektrona i GO fonona. Na osnovi ishoda numeričkog računa ovog i ranijih radova, izveli smo opća svojstva GO fononskih modova u sustavu n-slojne vezane kvantne jame. Ovaj se rad može smatrati poopćenjem prethodnih istraživanja.